Heliyon 10 (2024) e38851

Contents lists available at ScienceDirect

Heliyon

journal homepage: www.cell.com/heliyon

Research article

Network pharmacology and experimental study of Angelica sinensis and Astragalus membranaceus capsules in treating heart failure

Xue Wu [a,b,c,d], Ai Liu [a,c], Xinfang Lv [a,c,e], Xiaodong Zhi [a,c,e], Xiangting Zeng [d,f], Kai Liu [a,c,e], Xinke Zhao [a,c,e], Bing Jiang [a], HuGang Jiang [a,c], Yingdong Li [a,c,e,*]

[a] College of Integrated Traditional Chinese and Western Medicine, Gansu University of Chinese Medicine, Lanzhou, China
[b] Department of Cardiology, The Second Hospital of Lanzhou University, Lanzhou, China
[c] Key Laboratory of Prevention and Treatment for Chronic Diseases by Traditional Chinese Medicine, Affiliated Hospital of Gansu University of Chinese Medicine, Lanzhou, China
[d] The Second Clinical Medical School, Lanzhou University, Lanzhou, China
[e] Affiliated Hospital of Gansu University of Chinese Medicine, Lanzhou, China
[f] Department of General Surgery,The Second Hospital of Lanzhou University, Lanzhou, China

ARTICLE INFO

Keywords:
Network pharmacology
Molecular docking
Angelica sinensis and Astragalus membranaceus capsule
Heart failure

ABSTRACT

Objective: This study explores the mechanism of AAC in intervening heart failure (HF) using network pharmacology, molecular docking, and in vitro experimental validation.
Methods: The "active component-target" network and the "drug-disease target" protein interaction network were constructed using Cytoscape 3.9.0 and STRING Database. GO and KEGG enrichment analysis was performed using DAVID database. Then, the molecular docking of major compounds and target proteins was carried out using Autodock 1.5.7, and visualized with PyMOL 2.4.0 software. Finally, in vitro experimental validation was performed to explore the potential targets of AAC in treating HF.
Results: The study revealed significant targets implicated in a variety of GO bioprocess programs and KEGG signaling networks. The primary chemicals to have strong binding ability with target proteins in molecular docking, with quercetin having the best binding energy with MAPK at −6.72 Kcal/Mol.Validation of cellular experiments showed that AAC might reduce the apoptosis that doxorubicin causes in AC16 cells by controlling the levels of PIK3CA, AKT1, and MAPK1.
Conclusion: This study preliminarily reveals that AAC can treat HF through multiple components and multiple targets by using network pharmacology, molecular docking, and experimental validation.

1. Introduction

Globally, the incidence of heart failure (HF) is increasing and has become a major public health problem. It is estimated that the prevalence of HF is expected to exceed 50 % of the global population [1]. In recent years, modern medicine has made remarkable

* Corresponding author.
E-mail address: lydj412@163.com (Y. Li).

https://doi.org/10.1016/j.heliyon.2024.e38851
Received 3 March 2024; Received in revised form 30 September 2024; Accepted 1 October 2024
Available online 4 October 2024
2405-8440/© 2024 The Authors. Published by Elsevier Ltd. This is an open access article under the CC BY-NC license (http://creativecommons.org/licenses/by-nc/4.0/).

progress in the prevention and treatment of HF; however, there is still a lack of ideal treatment strategies in terms of diuretic resistance, repeated hospitalizations, and decreased quality of life. Therefore, it's very important to search for drugs that can directly target pathophysiological alterations in HF and to study their mechanisms at a deeper level. Over the past decades, traditional Chinese medicine (TCM) has been playing an increasingly important role in clinical practice in China with its multi-directional, multi-target, and multi-mechanism characteristics, and low toxic side effects. TCM has significant advantages and broad prospects in the treatment of HF [2].

Angelica sinensis and Astragalus membranaceus capsules (AAC) is composed two Chinese medicines, *Angelica sinensis* (Oliv.) Diels. and *Astragalus abbreviatus* Kar. & Kir. (http://www.theplantlist.org), originates from ancient TCM formula of Danggui Buxue Tang (DBT), which is a widely used ancient formula with a long history. Both Angelica sinensis and Astragalus membranaceus in the formula are local herbs in Gansu Province, known for their blood-nourishing,and blood-activating properties. Studies have shown~~s~~ that DBT can eliminate abnormal aggregation of erythroid progenitor cells caused by melanoma [3], inhibit the proliferation and fibrosis of glomerular mesangial cells induced by high glucose [4], and alleviate vascular senescence in chronic intermittent hypoxia mice [5]. It is used not only for the treatment of haematological disorders, but also for the treatment of endocrine and cardiovascular diseases. Despite the long history of DBT's use, its active ingredients, potential target genes, and intrinsic mechanisms remain unknown. Studies of Danshen Decoction in heart failure are also scare.

Network pharmacology applies drug pharmacological mechanisms to biological networks to elucidate the relationships between

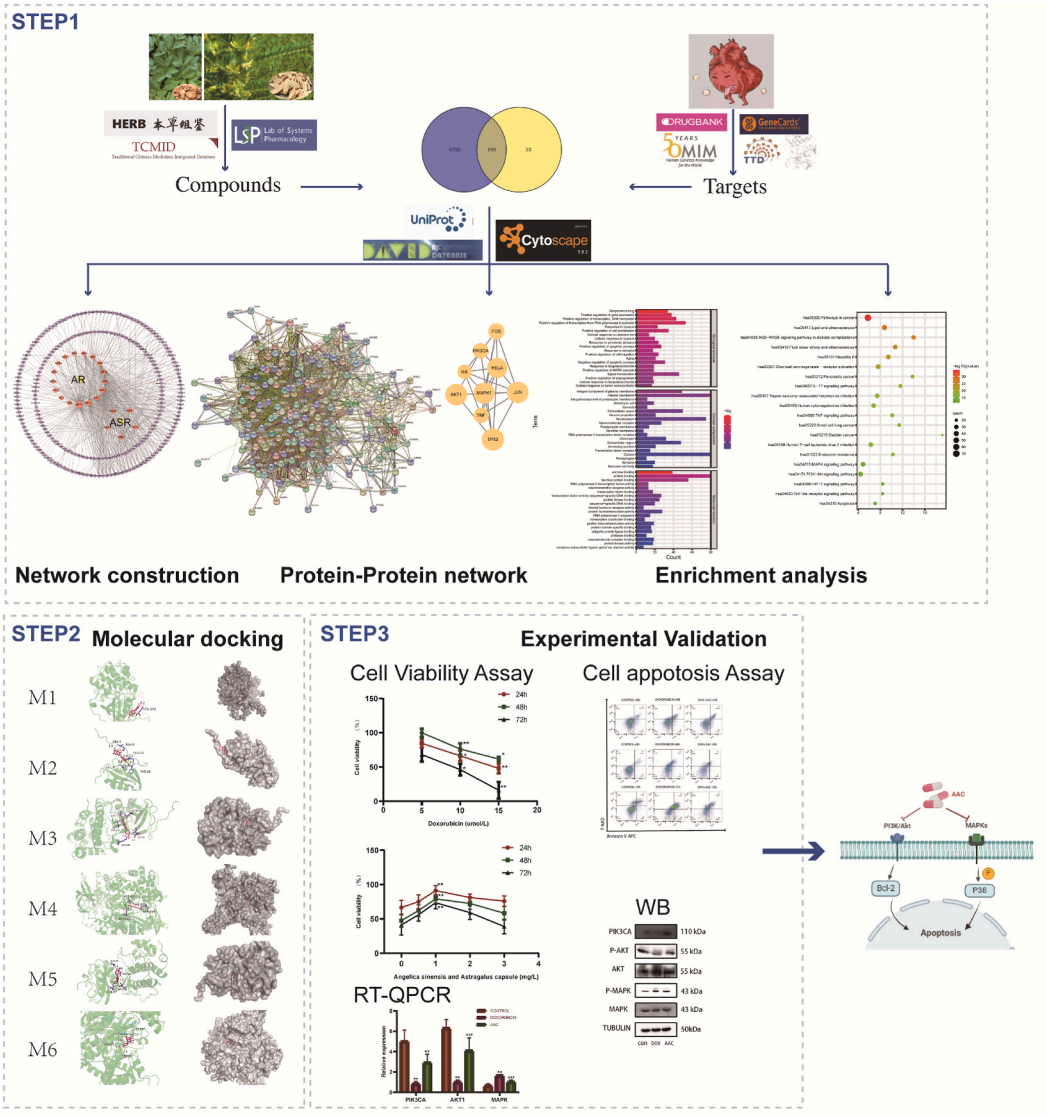

Fig. 1. Summary of the research performed in this research.STEP1: Network pharmacology analysis process; STEP2: Visualization of molecular docking; STEP3: Experimental verification results.

components, targets, and diseases [6]. It includes the develpoment of research networks based on databases, the identification of key substances and targets through network analysis [7], and the discovery of drug-gene-disease correlations [8]. Molecular docking is a theoretical approach to study the interactions and recognitions between protein receptors and small molecule ligands, predicting binding patterns and affinity strengths [9]. Therefore, network pharmacology and molecular docking provide new insights into the effective chemical selection and molecular mechanisms of traditional Chinese medicine [10]. Threfore, the present study employs a network pharmacology methods, combined with molecular docking and experimental validation in order to identify the active ingredients, expected targets, and mechanisms of AAC anti-hyperlipidemia. The workflow is shown in Fig. 1.

2. Materials and methods

2.1. Network pharmacology

2.1.1. Screening active compounds in AAC and predicting their targets

Compounds from AAC's Huangqi and Danggui originate from multiple open-access databases such as TCMID (Traditional Chinese Medicine Integrated,http://www.megabionet.org/tcmid/), Herb(http://herb.ac.cn/) [11], Chemistry Database (http://www.organchem.csdb.cn),TCMSP(Traditional Chinese Medicine Systems Pharmacology,https://tcmspw.com/tcmsp.php) [12]. The key words 'Astragalus' and 'Angelica sinensis' were used to retrieve active components, while we defined the screening criteria so that only those compounds that met the ADME criteria (OB>30 % and DL $\geq$ 0.18) [13,14]. In addition, the more studied active components were included based on existing literature reports. The targets of the above mentioned compounds were then identified from the database and finally combined and de-emphasized.

2.1.2. Constructing the "active compound-target" network of AAC

Using Cytoscape 3.9.0 software, an AAC "active compound-target" network was established, with nodes representing compounds or targets and edges representing their connections [15].

2.1.3. Identifying disease-related targets for HF

Heart failure related disease targets were retrieved from four public databases: GeneCards (https://www.genecards.org/) [16], DrugBank (https://go.drugbank.com/) [17], Therapeutic Target Database (TTD,http://db.idrblab.net/ttd/) [18],and Online Mendelian Inheritance in Man.

(OMIM,https://omim.org/) [19], using "heart failure" as the keyword. The results were consolidated to eliminate duplicates.

2.1.4. Constructing the protein-protein interaction (PPI) network and screening core targets

The PPI network was constructed by submitting overlapping target genes from AAC and HF to the String database (https://string-db.org/) [20]. The species was set as '*Homo sapiens*' and the minimum interaction threshold was set as 'highest confidence' (>0.09). The rest of the settings were set to the default settings to obtain the PPI network. Each node represents a protein, and each edge indicates a possible functional relationship between targets. These results were imported into Cytoscape for visualization, and the topological characteristics of key components were integrated.Using CytoNCA in Cytoscape 3.9.0 software, core targets were identified based on'degree','betweenness centrality' and 'closeness centrality'characteristics to screen the core target genes.

2.1.5. Network Gene Ontology (GO) and KEGG pathway enrichment

Using annotated, visualized, and integrated discovery database DAVID (https://david.ncifcrf.gov/),

Gene Ontology (GO) and KEGG pathway enrichment analysis were performed [21]. The intersection targets of illnesses and active substances were put into the David database, and Calculation settings such as "OFFICIAL-GENE-SYMBOL," "GENE List," and "Homo sapiens" were established. The enrichment findings for "biological process", "cellular component", "molecular function", and KEGG pathways were obtained. Furthermore, enrichment analysis was adjusted for all p values using the Benjamini-Hochberg technique, and the FDR for the first 20 revealed biological effect results was less than 0.05. Finally,the results were displayed as bubble charts using the online tool Microbiotics (http://www.bioinformatics.com.cn/).

2.2. Molecular docking

On the basis of the results of network pharmacology, key targets and candidate ingredients were selected to perform molecular docking. The mol2 format structures of the candidate ingredients were obtained from PubChem database, and the crystal structures of the key targets were obtained from PDB database. After removing water, adding polar hydrogen atoms, and extracting the ligand structureby using Pymol software, Using AutoDock 1.5.7 software to run 'autogrid', pick proteins and ligands. Chosing 'Genetic Algorithm', setting 'Number of Runs' to '50′ and 'Maximum Number of Generations' to '28000–30000'. Set 'Maximum Number of evals: medium' to '3000000′, output as 'Lamarckian', use 'AutoDock' for docking, and compute the binding energy. Finally, the PyMOL program was utilized for visualization.

2.3. Experimental verfication in vitro

2.3.1. Reagents and instruments

AAC (Lianzhenwei Pharmaceutical Co., Ltd., 20220802). The process of production is as follows: using the original ratio of 1:5 for Astragalus and Angelica sinensis, the mixture is boiled in water three times, impurities are filtered, the mixture is boiled and concentrated, and it is sent to the Gansu Province Membrane Institute of ceramic membrane microfiltration, where hollow fiber ultrafiltration membranes are selected, the molecular weight of its retention is 100 kDa (the technical parameters for the pressure of 0.5 k Pa•m^3, the pressure of 5–6 kg•m^{-3}, flow rate of 100L/h•m^2, temperature of 25 °C), and the ultrafiltration solution is sprayed, dried into a powder, and then loaded into capsules (National Food and Health: G20140331).Doxorubicin (Solarbio, Beijing, 620R021), PIK3CA, p-AKT1, AKT1, MAPK, p-MAPK, Tubulin antibodies (Affinity, Jiangsu, AF4669, AF0832, AF0836, BF8051, AF4001, AF7010), reverse transcription, RT-qPCR kits (Shanghai Yisheng, HB210716, HB220402), RNA extraction kit (Beijing Tengen, 4992562), flow cytometry (BriCyte E6), electrophoresis, transmittance instrument (American Bio-Rad), gel imaging analysis system (American AZUREc600), enzyme labeling instrument (Swiss infinite m200), reverse transcription instrument (Hangzhou Bioer), qPCR instrument (American Quantstudio).

2.3.2. Cell culture and model Establishment

Human cardiomyocytes AC16 were purchased from Guangzhou Saiku Biotechnology Co., Ltd. (Guangzhou, China,CC4030), and cultured in Dulbecco's Modified Eagle's Medium containing 12.5 % fetal bovine serum and 1 % penicillin-streptomycin at 5 % CO_2 humidity. The AC16 cells were treated with doxorubicin to simulate cardiotoxicity [22,23]. AC16 cells were seeded into 96-well plates, with three replicates per group. The cells were treated with different concentrations of doxorubicin (5, 10, 15 μmol/L) for 24, 48, and 72 h. After treatment, CCK-8 solution was added to AC16 for 1–2 h, and the absorbance value was measured to calculate the IC50 concentration of doxorubicin, screening out the optimal concentration.

2.3.3. Cell viability assay

AC16 cells were randomly divided into CONTROL, DOXORUBICIN, and AAC groups. The CONTROL group represented normal cultured AC16 cells, the DOXORUBICIN group received doxorubicin treatment, and the DOX + AAC group consisted of doxorubicin plus different concentrations of AAC (0.5, 1, 2, and 3 mg L^{-1}), treated for 24, 48, and 72 h. The cells were processed in the same manner as before, and the absorbance value was measured to screen out the optimal concentration of Angelica and Astragalus capsules.

2.3.4. Cell apoptosis detection using a flow cytometer

Apoptosis rate detection was performed using the Annexin V-FITC/PI double-labeling method. AC16 cells were divided into three groups: CONTROL, DOXORUBICIN (the optimal concentration selected in 2.3.3), and DOX + AAC (the optimal concentrations of doxorubicin and AAC). Cells were cultured for 24, 48, and 72 h, respectively, and then digested and collected. The cells were stained with Annexin V-APC/7-AAD kit. Analysis was conducted using FlowJoTMvX software.

2.3.5. Real-time Quantitative polymerase Chain Reaction (RT-qPCR)

Total RNA was extracted according to the manufacturer's instructions using an RNA extraction kit, and cDNA was generated using HiScript® II QRT SuperMix kit. The expression levels of PIK3CA, AKT1, MAPK1, and GAPDH mRNA were detected using a qPCR kit. All results were evaluated using the $2^{-\Delta\Delta Ct}$ technique. Primer sequences are shown in Table 1.

2.3.6. Western blot analysis

Post-intervention AC16 cells were precooled and washed with PBS, followed by protein extraction using lysis buffer. The concentration was calculated using the BCA technique, with 30 ng of protein loaded for SDS-PAGE electrophoresis, PVDF membrane transfer, blocking, and washing. The primary antibody was incubated overnight at 4 °C (Tublin 1:10000 dilution; MAPK1 1:5000 dilution; PIK3CA, AKT1, p-AKT1, p-MAPK1 1:1000 dilution), and the secondary antibody was incubated at room temperature for 2 h with TBST washing. ECL chemiluminescence technology and a gel imaging system were used for exposure, with Tublin as an internal reference. The target protein expression levels were assessed using Image J software.

Table 1
qPCR primer sequences.

Gene	Sequences
Gapdh-forward	CATGGCCTCCAAGGAGTAAGAC
Gapdh-reverse	AGGGTCTCTCTCTTCCTCTTGTG
MAPK1-forward	CTAGCAGAGATACGCAGACATTGTG
MAPK1-reverse	CCAAGAGCAGAAGGAATGAGTGTG
PI3KCA-forward	CGGTGACTGTGTGGGACTTATTG
PI3KCA-reverse	TGATGTAGTGTGTGGCTGTTGAAC
AKT1-forward	AGGATGTGGACCAACGTGAGG
AKT1-reverse	GCAGGCAGCGGATGATGAAG

2.4. Statistical analysis

Continuous Data were expressed as mean ± standard deviation. Intergroup differences were analyzed by one-way analysis of variance (ANOVA) using SPSS 23.0 software, and charts were drawn using Prism 8.0 software. The differences were considered statistically significant when $P < 0.05$.

3. Results

3.1. Active components and targets of AAC

AAC was composed of Radix Astragali and Radix Angelica sinensis. ADME screening (OB ≥ 30, DL ≥ 0.18) was conducted via searching in four databases and literature reports. A total of 22 active ingredients were collected, of which Radix Astragali contains 17 compounds, and Radix Angelica sinensis contains 5 compounds, as shown in Table 2.

3.2. Construction and analysis of AAC "active component-target" network

Using Cytoscape 3.9.0, the relationship network of AAC active components and their target interactions were drawn and analyzed, obtaining 254 nodes (including 232 targets and 22 active components) and 542 relationship lines, See Fig. 2.

3.3. Acquisition of heart failure targets

By seraching the GeneCards, OMIM, TTD, and DrugBank databases for relavent studies, targets closely related targets to the occurrence and development of HF were obtained. The Venn diagram showed that 199 targets meeting AAC and HF-related criteria were collected as potential AAC anti-HF targets, See Fig. 3.

3.4. Construction of protein-protein interaction (PPI) network and core target extraction

The disease targets of HF and the active component targets of AAC were intersected to obtain 199 common targets. After being imported into the String database, a PPI network with 198 nodes and 3468 edges was created, as shown in Fig. 4. Through the selection with "highest confidence (0.09)", 198 nodes and 705 edges were obtained. Using CytoNCA in Cytoscape 3.9.0 software, core targets

Table 2
Active compounds in AAC.

No.	Molecule Name	OB (%)	DL	Herb
AR1	Mairin	55.38	0.78	*Astragali*
AR2	Jaranol	50.83	0.29	*Astragali*
AR3	Hederagenin	36.91	0.75	*Astragali*
AR4	(3S,8S,9S,10R,13R,14S,17R)-10,13-dimethyl-17-[(2R,5S)-5-propan-2-yloctan-2-yl]-2,3,4,7,8,9,11,12,14,15,16,17-dodecahydro-1H-cyclopenta [a]phenanthren-3-ol	36.23	0.78	*Astragali*
AR5	Isorhamnetin	49.6	0.31	*Astragali*
AR6	3,9-di-O-methylnissolin	53.74	0.48	*Astragali*
AR7	7-O-methylisomucronulatol	74.69	0.3	*Astragali*
AR8	9,10-dimethoxypterocarpan-3-O-β-D-glucoside	36.74	0.92	*Astragali*
AR9	(6aR,11aR)-9,10-dimethoxy-6a,11a-dihydro-6H-benzofurano [3,2-c]c hromen-3-ol	64.26	0.42	*Astragali*
AR10	Bifendate	31.1	0.67	*Astragali*
AR11	Formononetin	69.67	0.21	*Astragali*
AR12	Calycosin	47.75	0.24	*Astragali*
AR13	Kaempferol	41.88	0.24	*Astragali*
AR14	FA	68.96	0.71	*Astragali*
AR15	Isomucronulatol-7,2′-di-O-glucosiole	49.28	0.62	*Astragali*
AR16	1,7-Dihydroxy-3,9-dimethoxy pterocarpene	39.05	0.48	*Astragali*
AR17	Quercetin	46.43	0.28	*Astragali*
ASR1	β-sitosterol	36.91	0.75	*Angelica sinensis*
ASR2	Stigmasterol	43.83	0.76	*Angelica sinensis*
ASR3	Ferulic Acid (CIS)[a]	54.97	0.06	*Angelica sinensis*
ASR4	Cis-ligustilide[a]	51.3	0.07	*Angelica sinensis*
ASR5	6,7,3′,8′-diligustilide[a]	9.83	0.7	*Angelica sinensis*

OB: oral bioavailability; DL: drug-likeness.
[a] Supplemental Literature Search.

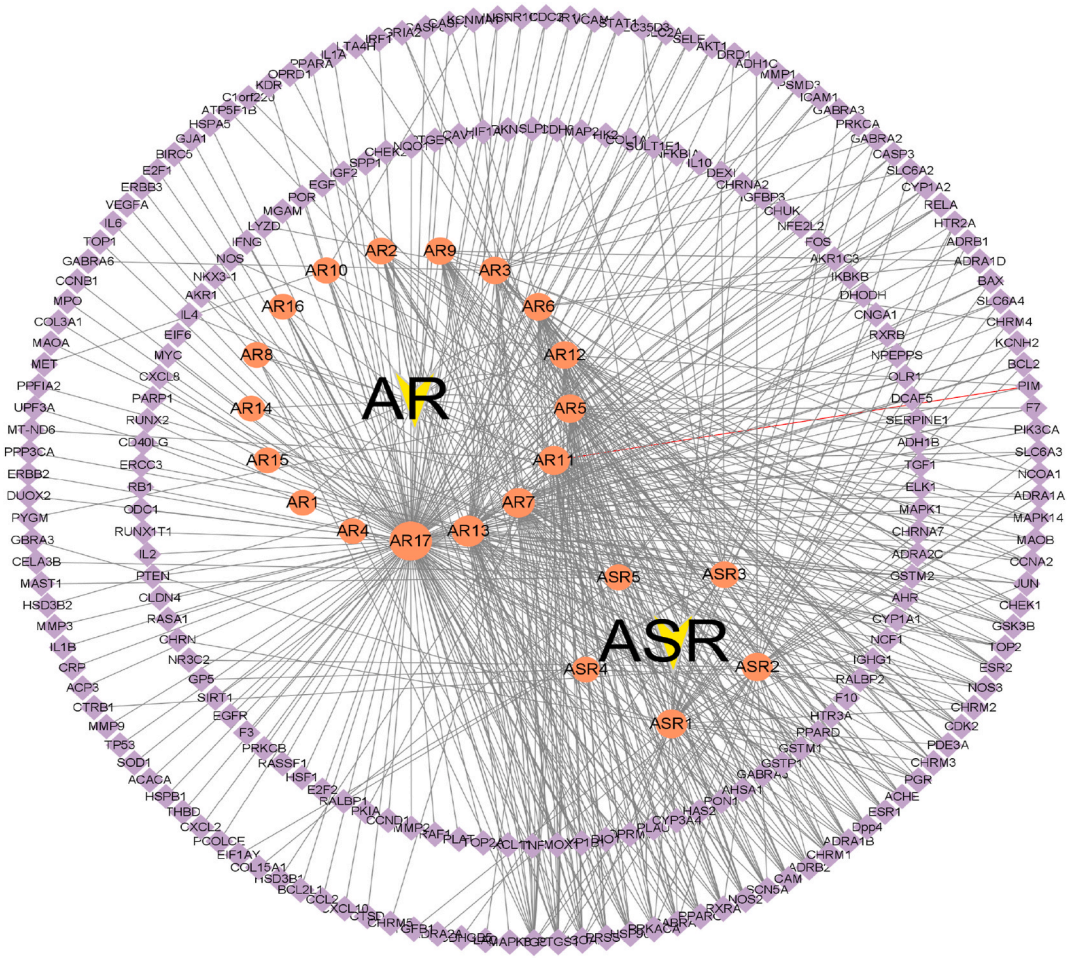

Fig. 2. AAC "Active Component-Target" Network. Red circles represents an active ingredient in ACC, The purple diamond represents the targets, and area represents the size of the degree value; AR stands for *Astragali*, ASR stands for *Angelica sinensis*, and the corresponding components are shown in Table 2. (For interpretation of the references to color in this figure legend, the reader is referred to the Web version of this article.)

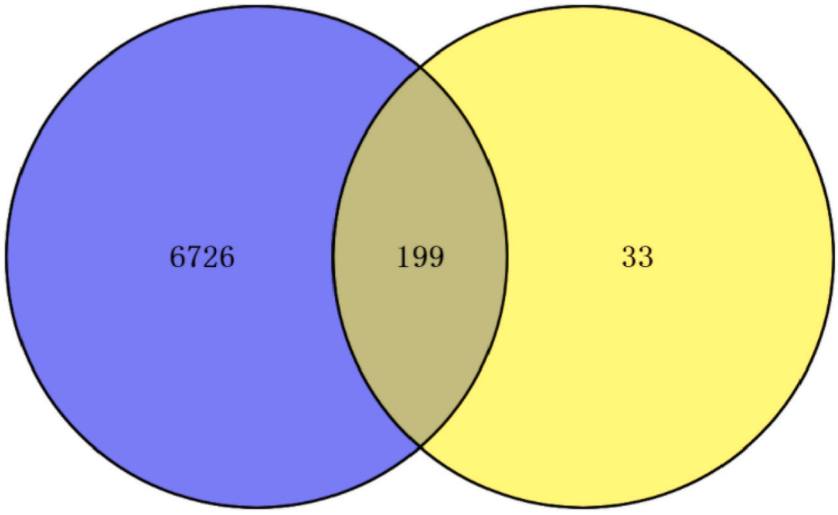

Fig. 3. The distribution of disease and therapeutic targets. Targets for diseases are shown in purple circles, whereas medication targets are shown in yellow circles. (For interpretation of the references to color in this figure legend, the reader is referred to the Web version of this article.)

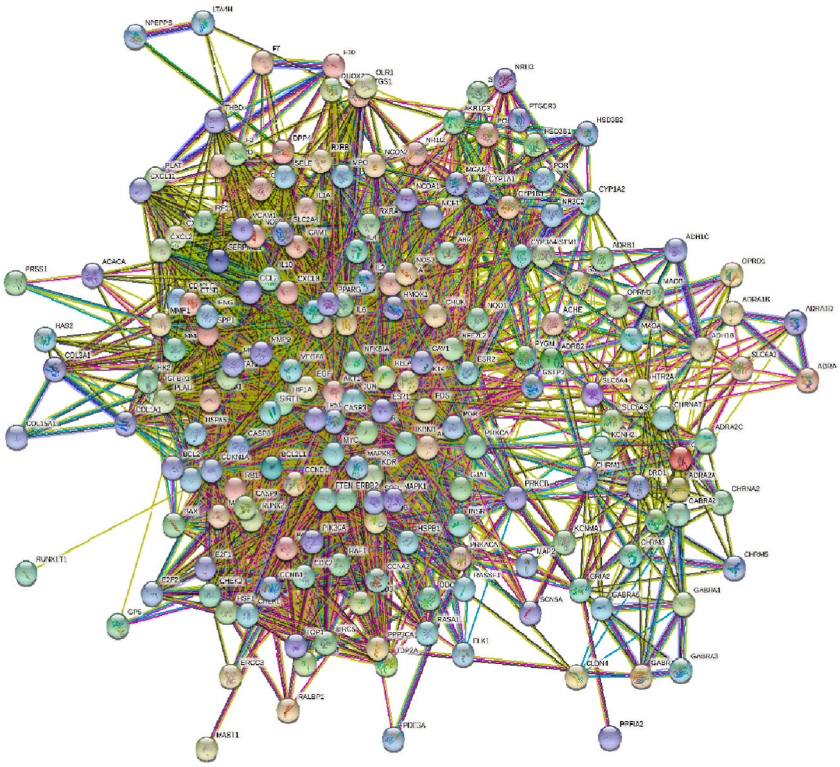

Fig. 4. PPI of AAC and HF.
Circles in different colors indicate targets.
More lines indicate higher enrichment target.

were searched based on “degree”, “degree interval”, and “closeness” characteristics; nodes with larger degree values indicate higher importance, as shown in Fig. 5. The results showed that the core targets include TP53, AKT1, JUN, MAPK1, RELA, FOS, PIK3CA, TNF, and IL6, which may play roles in AAC.

3.5. Visualization of GO function and KEGG enrichment analysis in AAC treatment of heart failure

We performed GO function and KEGG enrichment analysis on the 199 common targets using the David database. A total of 1209 GO functions were discovered, including 840 biological processes (BP) such as “Response to drug”,“Positive regulation of gene expression”,“transcription”, “DNA−templated and RNA polymerase II promoter”, 199 cellular components (CC) such as “Integral component of plasma membrane, presynaptic membrane”,“Membrane raft”,“Neuron projection” and 170 molecular functions (MF) such as “enzyme binding”,“protein binding”,“identical protein binding”,“neurotransmitter receptor activity”. The top 20 Log10(P) values were plotted as a bar chart with colors ranging from blue to red reflecting the increasing Log10(P) values, and the horizontal axis displays the number of key nodes (Fig. 6A).

KEGG enrichment analysis indicated 182 statistically significant pathways. Fig. 6B shows the results of bubble plot drawn using an online tool (http://www.bioinformatics.com.cn/), displaying the top 20 significantly enriched pathways with the highest gene counts. The study showed that the targets of AAC in treating HF are mainly concentrated in pathways such as IL-17, MAPK, PI3K-Akt signaling, endocrine resistance, Kaposi’s sarcoma-associated herpesvirus infection, and cell apoptosis. These results indicate that AAC can play a crucial role in the treatment of HF through multiple pathways.

The high enrichment for the PI3K-Akt signaling pathways GO and KEGG databases suggests that AAC may act via this pathways in the treatment of HF. We visualized the KEGG pathways in Fig. 7.

The bubble color diagram ranges from red to green, representing the Log10(*P*) values decreasing to increasing, and the bubble area represents the gene count of the pathway. The horizontal axis represents the enrichment of the pathway.

3.6. Analysis of molecular docking results

From the component-target network diagram, the high-degree components in Astragalus are quercetin, kaempferol,7-O-methylisomucronulato,formononetin, while in Angelica sinensis,it was Stigmasterol and beta-sitosterol. The core targets extracted from the PPI network include MAPK1, AKT1, PIK3CA, JUN, TP53, RELA, and FOS. Molecular docking was performed for each active

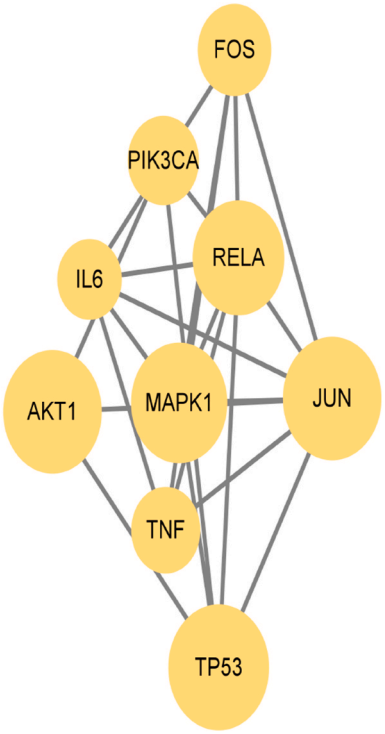

Fig. 5. Diagram of core targets.
The yellow circle is the extracted core and the larger the diameter of the circle, the larger the "degree value".

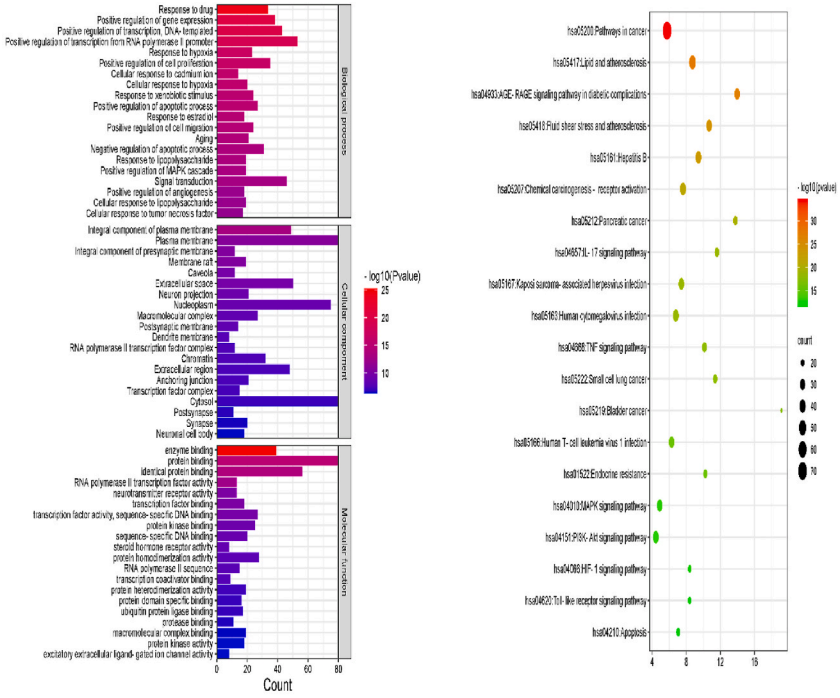

A. Most Enriched GO Terms **B. KEGG Pathway**

Fig. 6. Enrichment analysis. $p < 0.05$ as statistically significant.

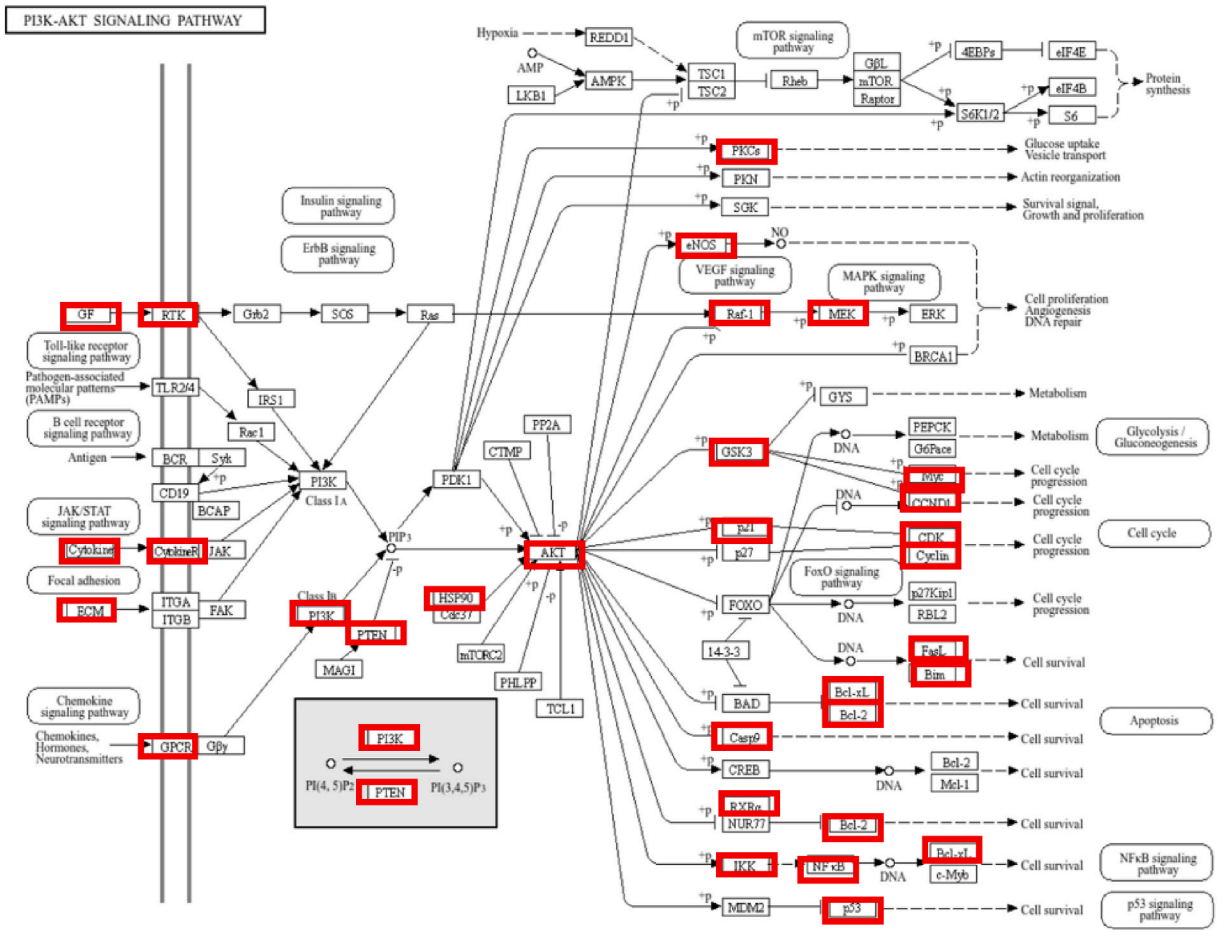

Fig. 7. Distribution of key targets in the PI3K/AKT signaling pathway.
The red rectangle stands for the key targets. The putative targets and the genes implicated in the pathway are shown in red.

component and target (Fig. 8).In molecular docking, a binding energy less than 0 indicates that binding can occur under natural conditions, and the lower the binding energy, the more stable the binding conformation. Small molecule compounds are more likely to interact with proteins, and a binding energy less than −5.0 kcal/mol suggests strong binding activity [22]. As shown in Table 3, the molecular docking results indicate that formononetin, quercetin,7-O-methylisomucronulato,kaempferol, stigmasterol and beta-sitosterol have binding energies less than −5, indicating good binding activity with the core target proteins. Among them, quercetin and kaempferol exhibit the highest activity, with quercetin having the optimal binding energy of −6.72 kcal/mol to MAPK.

3.7. CCK8 assay for cell viability

AC16 cells were cultured with different concentrations of doxorubicin (5 μmol/L, 10 μmol/L, 15 μmol/L) for 24h, 48h, and 72h, and the OD values were detected. The results showed that 15 μmol/L doxorubicin treatment for 48h was the optimal concentration for IC50 ($p < 0.01$), as shown in Fig. 9.

AC16 cells were divided into doxorubicin treatment groups (15 μmol) and 15μmol/Lol/L doxorubicin + different concentrations of AAC groups (0.5 mg•L^{-1}, 1 mg•L^{-1}, 2 mg•L^{-1}, 3 mg•L^{-1} AAC pretreatment for 2h), and the OD values were detected after 48h. The results suggested that cell viability was better at 15μmol/Lol/L doxorubicin + AAC 1 mg•L^{-1} ($p < 0.01$), see Fig. 10.

3.8. Flow cytometry for cell apoptosis

At 24h and 48h, compared with the control group, the apoptosis rate of AC16 cells increased ($p < 0.01$); compared with the DOX group, the apoptosis rate of AC16 cells decreased ($p < 0.01$) when given 1 mg•L^{-1} AAC; at 72h, the apoptosis and death rates of DOX and AAC groups were higher than the control group, and the apoptosis and death rates of AAC group were higher than the control group ($p < 0.01$). It can be seen that at 48h, the damage effect of doxorubicin on AC16 cells was the most significant, and the effect was the best when given 1 mg•L^{-1} AAC (Figs. 11 and 12).

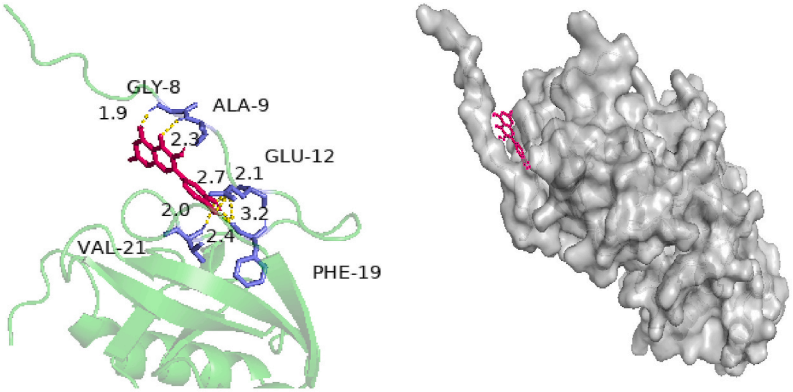

(A) Quercetin—MAPK1（ΔG =-6.72）

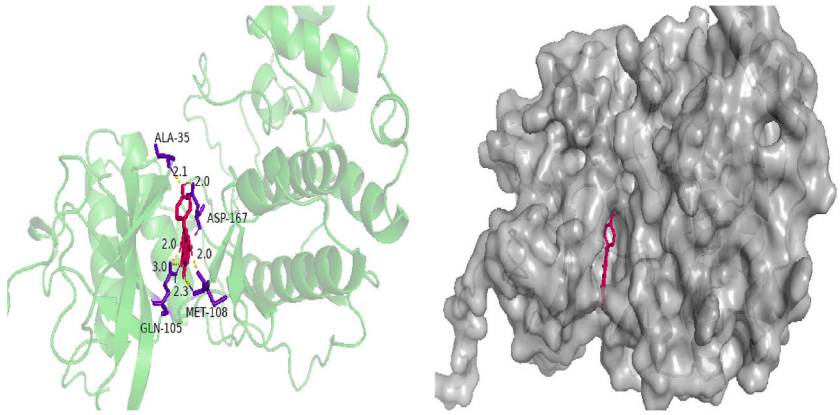

(B) Kaempferol—MAPK1（ΔG =-6.28）

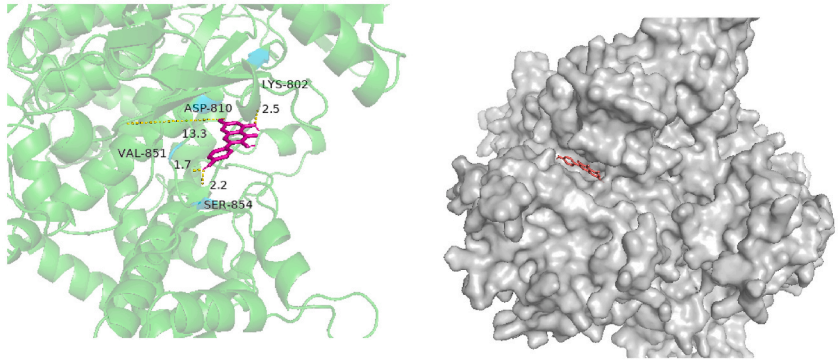

(C) Kaempferol—PIK3CA（ΔG =-6.15）

Fig. 8. Molecular docking analysis.
Left: two-dimensional image; Right: three-dimensional image. Proteins are shown in green and grey, active ingredients in red.
(A)The optimal binding modes of Quercetin and MAPK1 (ΔG = −6.72 kcal/mol).
(B)The optimal binding modes of Kaempferol and MAPK1 (ΔG = −6.28 kcal/mol).
(C)The optimal binding modes of Kaempferol and PIK3CA (ΔG = −6.15 kcal/mol).
(D)The optimal binding modes of 7-O-methylisomucronulatol and AKT1 (ΔG = −6.18 kcal/mol).
(E)The optimal binding modes of Formononetin and MAPK1 (ΔG = −6.43 kcal/mol).
(F)The optimal binding modes of Formononetin and PIK3CA (ΔG = −7.15 kcal/mol).

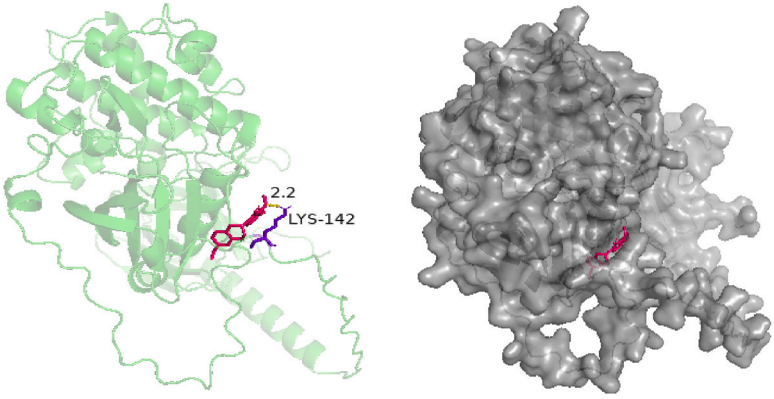

(D) 7-O-methylisomucronulatol—AKT1（ΔG =-6.18）

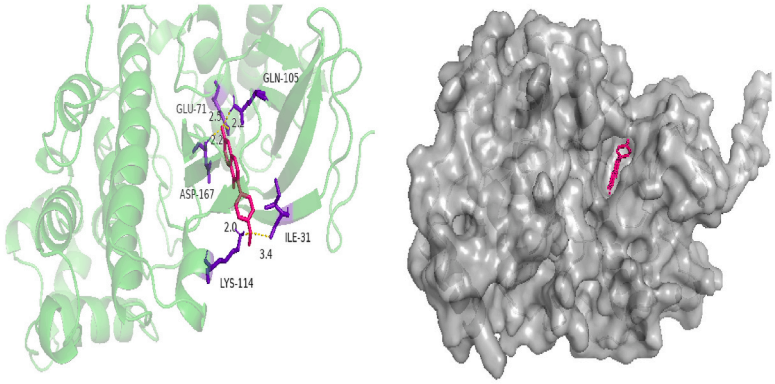

(E) Formononetin—MAPK1（ΔG =-6.43）

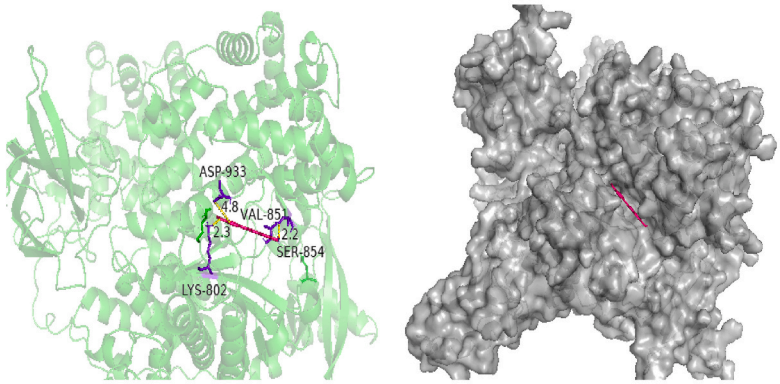

(F) Formononetin—PIK3CA（ΔG =-7.15）

Fig. 8. (*continued*).

3.9. Observation of Cell Morphology change under inverted microscope

The morphology and growth of control, DOXORUBICIN, and AAC groups were observed under an inverted microscope. As shown in Fig. 13, the cell morphology of the DOXORUBICIN group changed from spindle-shaped to round and small, with irregular edges, deformed and broken cell nuclei. The cell damage was severe compared with the control group, with a large number of floating dead cells appeared in the culture medium,and the cell damage was reduced in the AAC group compared with the DOXORUBICIN group than that.

Table 3
Docking energy.

Molecule name	Docking energy (Kcal/Mol)						
	MAPK1	AKT1	PIK3CA	JUN	TP53	RELA	FOS
Quercetin	−6.72	−5.68	−5.91	−4.17	−5.38	−4.3	−3.83
Kaempferol	−6.28	−5.88	−6.15	−4.58	−4.8	−4.29	−3.63
7-O-methylisomucronulatol	−6.07	−6.18	−5.89	−4.78	−5.39	−5.13	−3.71
Formononetin	−6.11	−5.23	−6.11	−4.05	−4.76	−5.59	−3.87
Stigmasterol	−5.51	−5.5	−6.06	−4.14	−5.16	−4.75	−3.73
Beta-sitosterol	−5.86	−6.09	−6.04	−4.39	−5.11	−4.73	−3.74

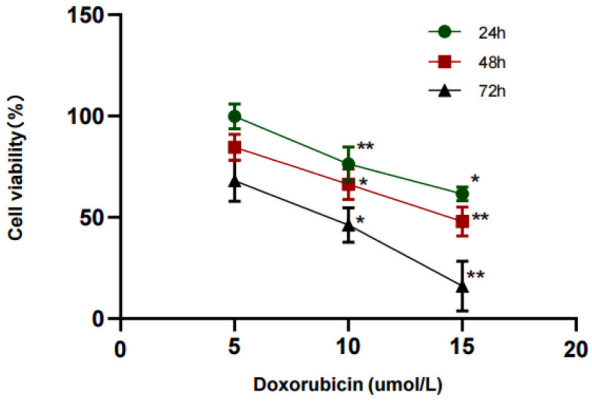

Fig. 9. CCK assay for cell viability
Vertical axis indicates cell viability, horizontal axis indicates different doses of doxorubicin. Different colors represent different times. Comparatively to 5 μmol/L doxorubicin,*$p < 0.05$; **$p < 0.01$. (For interpretation of the references to color in this figure legend, the reader is referred to the Web version of this article.)

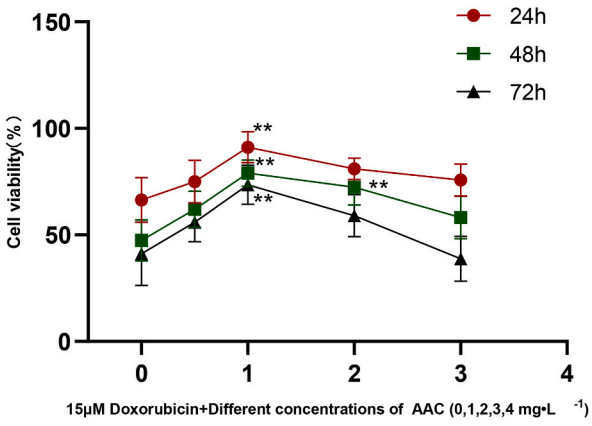

Fig. 10. CCK assay for cell viability
Vertical axis indicates cell viability, horizontal axis indicates 15 μmol/L doxorubicin + different concentrations of AAC. Different colors represent different times.
0 mg•L^{-1} AAC:Only 15 μmol/L is given; Comparatively to 0 mg•L^{-1} AAC group, **$p < 0.01$. (For interpretation of the references to color in this figure legend, the reader is referred to the Web version of this article.)

3.10. RT-qPCR analysis

Compared with the control group, the mRNA levels of PIK3CA and AKT1 in the DOXORUBICIN group decreased, while the level of MAPK1 increased ($p < 0.01$); after giving 1 mg•L^{-1} AAC, the expression of PIK3CA and AKT1 increased ($p < 0.05$), and the level of MAPK1 decreased ($p < 0.01$), see Fig. 14.

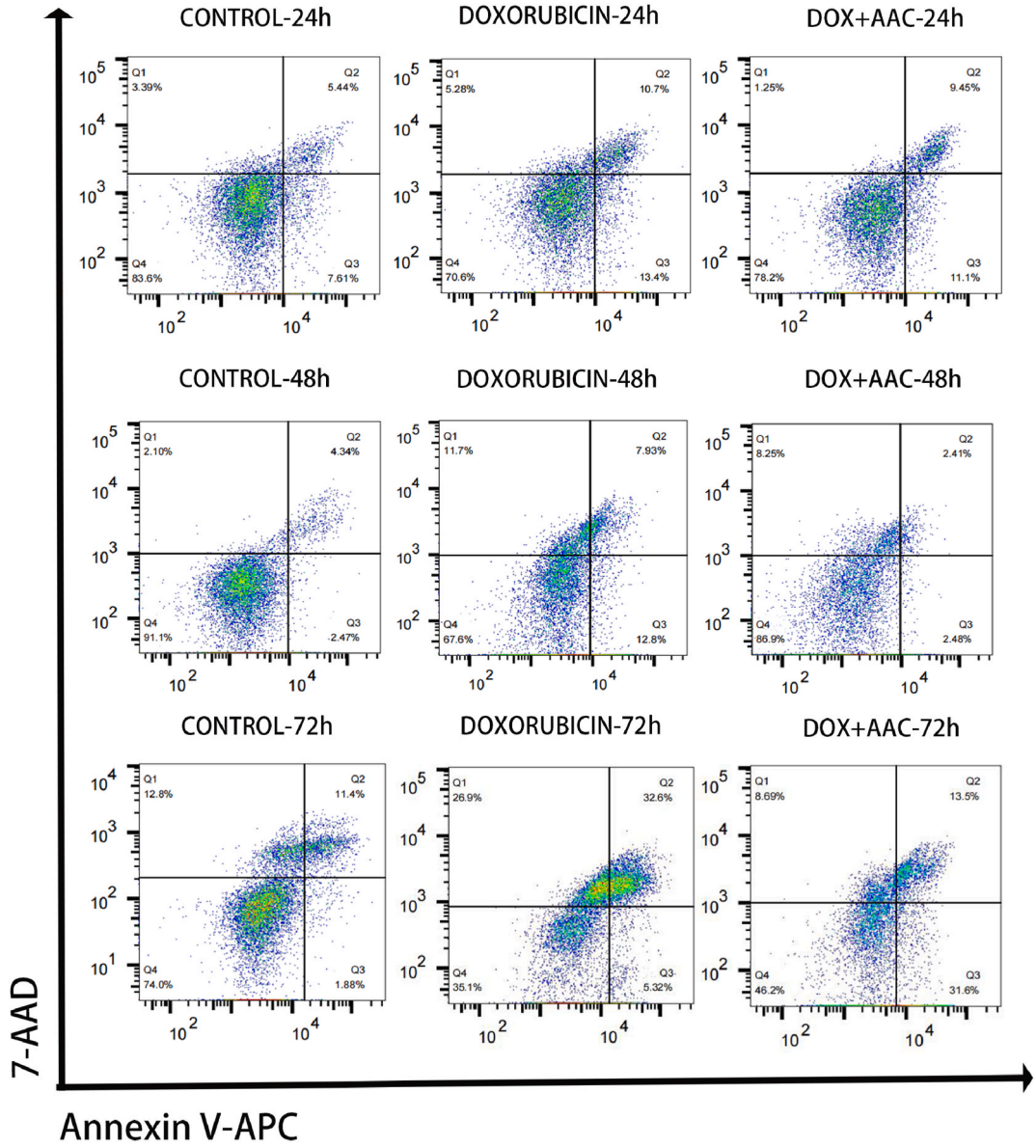

Fig. 11. Flow cytometry detection of apoptosis.

3.11. Western Blot analysis

Compared with the control group, the levels of p-MAPK1/MAPK1 increased in the DOXORUBICIN group, while the levels of PIK3CA and p-AKT1/AKT1 decreased ($p < 0.01$). The 1 mg•L^{-1} AAC treatment group resulted in increased expression of PIK3CA and p-AKT1/AKT1, and decreased expression of p-MAPK1/MAPK1 ($p < 0.01$), see in Fig. 15.

4. Discussion

Heart failure (HF) affects millions of adults worldwide, with a poor prognosis. Approximately half of patients diagnosed with HF die within 5 years [23]. Traditional Chinese Medicine (TCM) views HF as a disease characterized by essential deficiency and manifestation, with underlying yang deficiency and concurrent yin deficiency, blood stasis as the manifestation [24]. Professor Li Yingdong, the leader of our project and a renowned TCM physician, believes that qi deficiency and blood stasis are prevalent throughout the entire disease progression of HF. The treatment approach advocates warming the yang, promoting blood circulation, and draining fluids, focusing on supporting the healthy and eliminating the pathogenic, with emphasis on warming the yang and boosting qi, and promoting blood circulation and resolving stasis. AAC are local herbs in Gansu Province and are used in TCM. Angelica sinensis [25] is

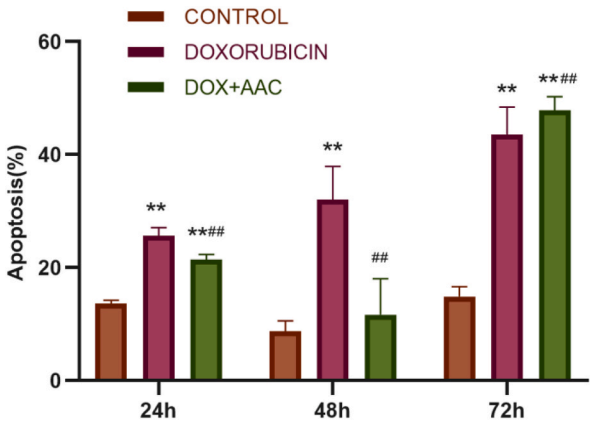

Fig. 12. Apoptosis Rate in each group.
Different colors for different groups.Comparatively to CONTROL group, $*p < 0.05$;$**p < 0.01$; Comparatively to DOXORUBICIN group,$^{\#}p < 0.05$;$^{\#\#}p < 0.01$.

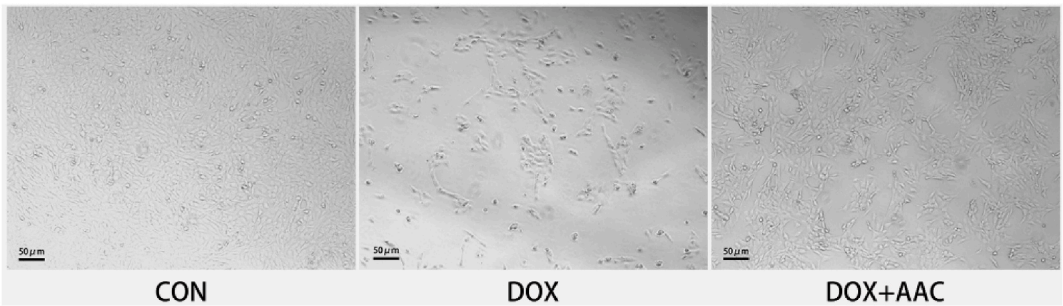

Fig. 13. Observation of cell morphology.

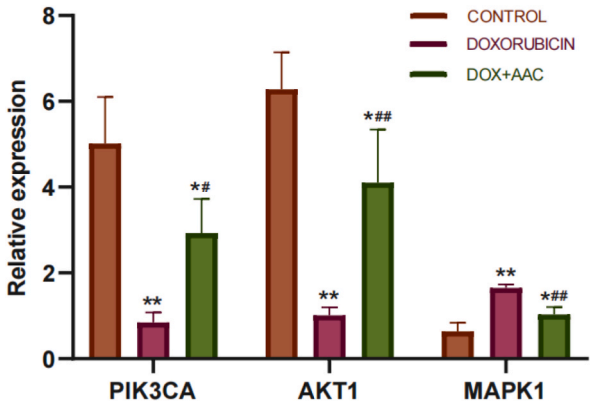

Fig. 14. Expression of PIK3CA, AKT1, MAPK1 mRNA.
Different colors for different groups. Comparatively to CONTROL group, $*p < 0.05$;$**p < 0.01$; Comparatively to DOXORUBICIN group,$^{\#}p < 0.05$;$^{\#\#}p < 0.01$.

sweet, warm, and enters the liver, heart, and spleen channels, capable of nourishing blood and promoting blood circulation. Astragalus membranaceus [26] is sweet, warm, and enters the lung and spleen channels, exhibiting effects of tonifying qi and boosting Yang. Combining the two together can not only replenish the spleen and stomach qi but also promote blood circulation and remove pathogenic factors, conforming to the TCM dialectics of treating chronic HF.

Our network pharmacology study revealed that AAC contain multiple active ingredients, such as formononetin, quercetin, 7-O-methylisomucronulato, kaempferol, stigmasterol, beta-sitosterol, calycosin and ferulic acid. Previous studies have shown that calycosin can inhibit myocardial fibrosis [27], ferulic acid have various pharmacological properties for the treatment of heart diseases [28,

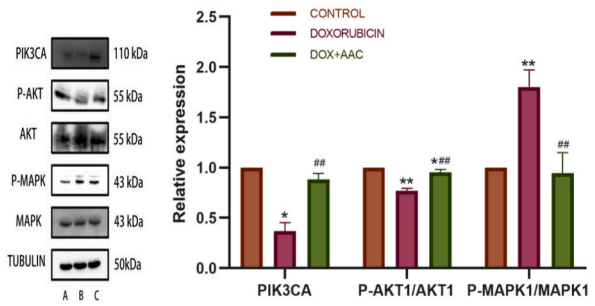

Fig. 15. Expression of PIK3CA, p-AKT1/AKT1, p-MAPK1/MAPK1 proteins.
A: CONTROL group; B:DOXORUBICIN group; C: DOX + AAC group.
Different colors for different groups. Comparatively to CONTROL group, $^{*}p < 0.05$;$^{**}p < 0.01$; Comparatively to DOXORUBICIN group,$^{\#}p < 0.05$;$^{\#\#}p < 0.01$.

29]. Formononetin significantly delayed the progression of atherosclerosis by inhibiting the adhesion and inflammation response of atherogenic monocytes [30,31]. Quercetin can significantly reduce rat heart toxicity induced by 5-FU [32] and inhibit ischemia/reperfusion injury in H9C2 cells [33]. β-sitosterol has benefits for anti-diabetes, cardioprotection, anticancer, antioxidant, and liver protection [34]. This is consistent with the active ingredients that we screened.

After constructing the PPI network and extracting the core targets, KEGG enrichment analysis revealed their significant involvement in the "MAPK signaling pathway" and "PI3K-Akt signaling pathway." Studies have shown that formononetin can regulate the PI3K/Akt/Nrf2 and PI3K/Akt/FoxO3a signaling pathways [35]. Quercetin can regulate MAPK [36] and PI3K/Akt pathways, reducing atherosclerosis [37]. Stigmasterol can inhibit the Akt/mTOR pathway, resulting in cancer cell autophagy and death [38].Kaempferol Inhibits Oxidative Stress and Apoptosis by Regulating Glucose Uptake, Mitochondrial Biogenesis via the PI3K/AKT and MAPK Signaling Pathways [39,40].This is consistent with our enrichment results.

We conducted molecular docking of the effective active ingredients and targets obtained from network pharmacology analysis, suggesting that the binding energies of beta-sitosterol, kaempferol, stigmasterol, formononetin, quercetin, and 7-O-methylisomucronulato with MAPK1, AKT1, and PIK3CA were all less than −5, with quercetin and kaempferol exhibiting the best binding. Quercetin inhibiting pyroptosis by ROS/MAPK/NF-kappaB pathway [41]. Kaempferol inhibited angiogenesis by suppressing HIF-1α and VEGFR2 activation through ERK/p38 MAPK and PI3K/Akt/mTOR signaling pathways in endothelial cells, which is consistent with the results of our network pharmacology and molecular docking. We thus speculate that AAC may alleviate heart failure through these active ingredients.

To validate the above conclusion, we performed in vitro experiments using human cardiomyocytes AC16. Many previous studies [42,43] have shown that DOX can cause heart failure, so we similarly constructed the heart failure model with DOX induction.We found that doxorubicin significantly increased cell apoptosis rate, decreased PIK3CA and AKT1 mRNA levels, and increased MAPK1 mRNA levels; decreased PIK3CA and p-AKT1/AKT1 protein levels, but increased p-MAPK1/MAPK1 protein levels. Administration of doxorubicin + AAC intervention significantly reduced AC16 cell apoptosis rate and altered mRNA and protein expression. This

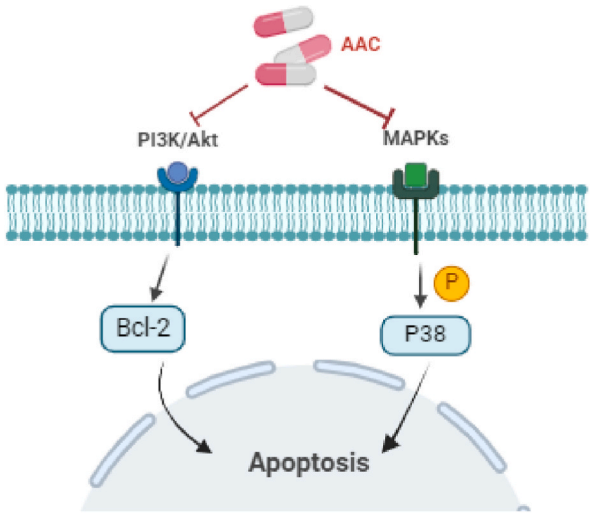

Fig. 16. Diagram of the mechanism of AAC treatment in heart failure.
AAC:Angelica sinensis and Astragalus membranaceus capsules. Orange indicates phosphorylation.

indicates that AAC alleviates doxorubicin toxicity to cardiomyocytes by upregulating PIK3CA, p-AKT1/AKT1 expression, and downregulating p-MAPK1/MAPK1 expression. This result validates the MAPK and PI3K-Akt pathways enriched in the pathway analysis and molecular docking. Our previous studies demonstrated that ACC can enhance cardiac function in heart failure animals via modulating the PI3K/AKT pathway [44]. Animal research by Cheng, Li, and others have shown that ACC might have a therapeutic function via modulating MAPK [45–47].Therefore, experimentally verified that AAC can effectively regulate PIK3CA, AKT1, and MAPK1 expression, which is beneficial for the treatment of heart failure,see in Fig. 16.Additionally, our study found that 7-O-methylisomucronulato and other active ingredients also have a better binding ability with targets, but no relevant literature studies have been seen yet. Our research group will continue to pay more attention and conduct the study in the follow-up research.

Cui [48] et al. used modified DBT to treat heart failure patients combined with anemia, finding that DBT could improve patients' symptoms, cardiac function, and quality of life. Similarly, Wen et al. [49] discovered that modified DBT replenishing soup provided substantial clinical effects in patients with chronic heart failure and anemia, such as alleviating symptoms and speeding up the treatment process. However, there have been few clinical studies published in English in recent years. This may be due to the complexity of the chemical preparation's composition, which has not been widely recognized worldwide. As a result, it is crucial to understand how it works.In the future research, we should make full use of cutting-edge technologies to further improve the isolation and identification of traditional Chinese medicine compounds, and clarify their mechanisms of action, and potential toxicities to provide a theoretical basis for their clinical application.

5. Conclusion

In this study, we employed network pharmacology, molecular docking, and in vitro experiments to validate the active ingredients of AAC and preliminary explore its mechanism in heart failure. Based on a multidisciplinary strategy, it provides a comprehensive and innovative approach to find traditional Chinese medicine active compounds, core target genes, and potential mechanisms for the treatment of diseases with a promising multidisciplinary approach.

Funding

This is research that has been provided by NSFC(32060231,82360926), The Science and Technology Department of Gansu Province (21JR7RA399, 23JRRA1642), the Major Science and Technology special project of Gansu Province (20ZD7FA002), Gansu Provincial Education Department unveils the project (2021jyjbgs-03),Gansu Province Traditional Chinese Medicine Prevention and Treatment of Major Diseases Special Project (ZGKZD-2018-02), The Lanzhou Science and Technology Bureau (2023-QN-191, 2018-ZD-1), and the Cuiying Scientific and Technological Innovation Program of Lanzhou University Second Hospital (CY2021-BJ-A17).

Data availability

Author can confirm that all relevant data are included in the article and/or its supplementary information files.

Ethical approval

This article does not contain any studies with human participants or animals performed by any of the authors.

Informed consent

This article does not contain any studies with human participants performed by any of the authors.

Consent for publication

All authors agree to public.

CRediT authorship contribution statement

Xue Wu: Writing – original draft. **Ai Liu:** Visualization, Formal analysis. **Xinfang Lv:** Validation. **Xiaodong Zhi:** Validation. **Xiangting Zeng:** Visualization, Data curation. **Kai Liu:** Visualization, Data curation. **Xinke Zhao:** Writing – review & editing, Project administration. **Bing Jiang:** Validation. **HuGang Jiang:** Visualization, Data curation. **Yingdong Li:** Writing – review & editing, Project administration.

Declaration of competing interest

The authors declare that they have no known competing financial interests or personal relationships that could have appeared to influence the work reported in this paper.

References

[1] P.A. Heidenreich, B. Bozkurt, D. Aguilar, L.A. Allen, J.J. Byun, M.M. Colvin, A. Deswal, M.H. Drazner, S.M. Dunlay, L.R. Evers, J.C. Fang, S.E. Fedson, G. C. Fonarow, S.S. Hayek, A.F. Hernandez, P. Khazanie, M.M. Kittleson, C.S. Lee, M.S. Link, C.A. Milano, L.C. Nnacheta, A.T. Sandhu, L.W. Stevenson, O. Vardeny, A.R. Vest, C.W. Yancy, AHA/ACC/HFSA guideline for the management of heart failure: a report of the American college of cardiology/American heart association joint committee on clinical practice guidelines, Circulation 145 (2022) e895–e1032, https://doi.org/10.1161/CIR.0000000000001063, 2022.

[2] Y. Xiang, Z. Guo, P. Zhu, J. Chen, Y. Huang, Traditional Chinese medicine as a cancer treatment: modern perspectives of ancient but advanced science, Cancer Med. 8 (2019) 1958–1975, https://doi.org/10.1002/cam4.2108.

[3] C. Li, F. Zhu, C. Xu, P. Xiao, J. Wen, X. Zhang, B. Wu, Dangguibuxue decoction abolishes abnormal accumulation of erythroid progenitor cells induced by melanoma, J. Ethnopharmacol. 242 (2019) 112035, https://doi.org/10.1016/j.jep.2019.112035.

[4] X.D. Ren, Y.W. Zhang, X.P. Wang, Y.R. Li, Effects of Dangguibuxue decoction on rat glomerular mesangial cells cultured under high glucose conditions, BMC Complement Altern Med 17 (2017) 283, https://doi.org/10.1186/s12906-017-1774-4.

[5] D. Li, J. Si, Y. Guo, B. Liu, X. Chen, K. Qi, S. Yang, E. Ji, Danggui-Buxue decoction alleviated vascular senescence in mice exposed to chronic intermittent hypoxia through activating the Nrf2/HO-1 pathway, Pharm. Biol. 61 (2023) 1041–1053, https://doi.org/10.1080/13880209.2023.2230753.

[6] Z. Yuan, Y. Pan, T. Leng, Y. Chu, H. Zhang, J. Ma, X. Ma, Progress and prospects of research ideas and methods in the network pharmacology of traditional Chinese medicine, J Pharm Pharm Sci 25 (2022) 218–226, https://doi.org/10.18433/jpps32911.

[7] T.T. Luo, Y. Lu, S.-K. Yan, X. Xiao, X.-L. Rong, J. Guo, Network pharmacology in research of Chinese medicine formula: methodology, application and prospective, Chin. J. Integr. Med. 26 (2020) 72–80, https://doi.org/10.1007/s11655-019-3064-0.

[8] C. Nogales, Z.M. Mamdouh, M. List, C. Kiel, A.I. Casas, H.H.H.W. Schmidt, Network pharmacology: curing causal mechanisms instead of treating symptoms, Trends Pharmacol. Sci. 43 (2022) 136–150, https://doi.org/10.1016/j.tips.2021.11.004.

[9] I.A. Vakser, Protein-protein docking: from interaction to interactome, Biophys. J. 107 (2014) 1785–1793, https://doi.org/10.1016/j.bpj.2014.08.033.

[10] S. Li, B. Zhang, Traditional Chinese medicine network pharmacology: theory, methodology and application, Chin. J. Nat. Med. 11 (2013) 110–120, https://doi.org/10.1016/S1875-5364(13)60037-0.

[11] S. Fang, L. Dong, L. Liu, J. Guo, L. Zhao, J. Zhang, D. Bu, X. Liu, P. Huo, W. Cao, Q. Dong, J. Wu, X. Zeng, Y. Wu, Y. Zhao, HERB: a high-throughput experiment- and reference-guided database of traditional Chinese medicine, Nucleic Acids Res. 49 (2021) D1197–D1206, https://doi.org/10.1093/nar/gkaa1063.

[12] R. Xue, Z. Fang, M. Zhang, Z. Yi, C. Wen, T. Shi, TCMID: traditional Chinese Medicine integrative database for herb molecular mechanism analysis, Nucleic Acids Res. 41 (2013) D1089–D1095, https://doi.org/10.1093/nar/gks1100.

[13] B.G. Giménez, M.S. Santos, M. Ferrarini, J.P.S. Fernandes, Evaluation of blockbuster drugs under the rule-of-five, Pharmazie 65 (2010) 148–152.

[14] S. Tian, J. Wang, Y. Li, X. Xu, T. Hou, Drug-likeness analysis of traditional Chinese medicines: prediction of drug-likeness using machine learning approaches, Mol. Pharm. 9 (2012) 2875–2886, https://doi.org/10.1021/mp300198d.

[15] D. Otasek, J.H. Morris, J. Bouças, A.R. Pico, B. Demchak, Cytoscape Automation: empowering workflow-based network analysis, Genome Biol. 20 (2019) 185, https://doi.org/10.1186/s13059-019-1758-4.

[16] G. Stelzer, N. Rosen, I. Plaschkes, S. Zimmerman, M. Twik, S. Fishilevich, T.I. Stein, R. Nudel, I. Lieder, Y. Mazor, S. Kaplan, D. Dahary, D. Warshawsky, Y. Guan-Golan, A. Kohn, N. Rappaport, M. Safran, D. Lancet, The GeneCards suite: from gene data mining to disease genome sequence analyses, Curr Protoc Bioinformatics 54 (2016), https://doi.org/10.1002/cpbi.5, 1.30.1-1.30.33.

[17] D.S. Wishart, Y.D. Feunang, A.C. Guo, E.J. Lo, A. Marcu, J.R. Grant, T. Sajed, D. Johnson, C. Li, Z. Sayeeda, N. Assempour, I. Iynkkaran, Y. Liu, A. Maciejewski, N. Gale, A. Wilson, L. Chin, R. Cummings, D. Le, A. Pon, C. Knox, M. Wilson, DrugBank 5.0: a major update to the DrugBank database for 2018, Nucleic Acids Res. 46 (2018) D1074–D1082, https://doi.org/10.1093/nar/gkx1037.

[18] Y. Wang, S. Zhang, F. Li, Y. Zhou, Y. Zhang, Z. Wang, R. Zhang, J. Zhu, Y. Ren, Y. Tan, C. Qin, Y. Li, X. Li, Y. Chen, F. Zhu, Therapeutic target database 2020: enriched resource for facilitating research and early development of targeted therapeutics, Nucleic Acids Res. 48 (2020) D1031–D1041, https://doi.org/10.1093/nar/gkz981.

[19] J.S. Amberger, A. Hamosh, Searching online mendelian inheritance in man (OMIM): a knowledgebase of human genes and genetic phenotypes, Curr Protoc Bioinformatics 58 (2017), https://doi.org/10.1002/cpbi.27, 1.2.1-1.2.12.

[20] D. Szklarczyk, A.L. Gable, D. Lyon, A. Junge, S. Wyder, J. Huerta-Cepas, M. Simonovic, N.T. Doncheva, J.H. Morris, P. Bork, L.J. Jensen, C. von Mering, STRING v11: protein-protein association networks with increased coverage, supporting functional discovery in genome-wide experimental datasets, Nucleic Acids Res. 47 (2019) D607–D613, https://doi.org/10.1093/nar/gky1131.

[21] D.W. Huang, B.T. Sherman, R.A. Lempicki, Systematic and integrative analysis of large gene lists using DAVID bioinformatics resources, Nat. Protoc. 4 (2009) 44–57, https://doi.org/10.1038/nprot.2008.211.

[22] K.Y. Hsin, S. Ghosh, H. Kitano, Combining machine learning systems and multiple docking simulation packages to improve docking prediction reliability for network pharmacology, PLoS One 8 (2013) e83922, https://doi.org/10.1371/journal.pone.0083922.

[23] S.S. Virani, A. Alonso, E.J. Benjamin, M.S. Bittencourt, C.W. Callaway, A.P. Carson, A.M. Chamberlain, A.R. Chang, S. Cheng, F.N. Delling, L. Djousse, M.S. V. Elkind, J.F. Ferguson, M. Fornage, S.S. Khan, B.M. Kissela, K.L. Knutson, T.W. Kwan, D.T. Lackland, T.T. Lewis, J.H. Lichtman, C.T. Longenecker, M.S. Loop, P.L. Lutsey, S.S. Martin, K. Matsushita, A.E. Moran, M.E. Mussolino, A.M. Perak, W.D. Rosamond, G.A. Roth, U.K.A. Sampson, G.M. Satou, E.B. Schroeder, S. H. Shah, C.M. Shay, N.L. Spartano, A. Stokes, D.L. Tirschwell, L.B. VanWagner, C.W. Tsao, American heart association council on epidemiology and prevention statistics committee and stroke statistics subcommittee, heart disease and stroke statistics-2020 update: a report from the American heart association, Circulation 141 (2020) e139–e596, https://doi.org/10.1161/CIR.0000000000000757.

[24] L. Chen, D. Yu, S. Ling, J.-W. Xu, Mechanism of tonifying-kidney Chinese herbal medicine in the treatment of chronic heart failure, Front Cardiovasc Med 9 (2022) 988360, https://doi.org/10.3389/fcvm.2022.988360.

[25] L. Cheng, M. Wang, Z. Zhang, F. Shao, Clinical efficacy of dangguibuxue decoction as an adjuvant therapy for diabetic nephropathy:a meta-analysis, Chinses General Pracitice 24 (2021) 3477–3483.

[26] X. Zhao, G. Xiang, J. Wang, J. Teng, Herbal textual research on efficacy, indications and contraindications of Danggui (Angelica), China Journal of Traditional Chinese Medicine and Pharmacy 35 (2020) 2479–2482.

[27] G. Chen, H. Xu, T. Xu, W. Ding, G. Zhang, Y. Hua, Y. Wu, X. Han, L. Xie, B. Liu, Y. Zhou, Calycosin reduces myocardial fibrosis and improves cardiac function in post-myocardial infarction mice by suppressing TGFBR1 signaling pathways, Phytomedicine 104 (2022) 154277, https://doi.org/10.1016/j.phymed.2022.154277.

[28] V.F. Salau, O.L. Erukainure, K.A. Olofinsan, N.Z. Msomi, O.K. Ijomone, M.S. Islam, Ferulic acid mitigates diabetic cardiomyopathy via modulation of metabolic abnormalities in cardiac tissues of diabetic rats, Fundam. Clin. Pharmacol. 37 (2023) 44–59, https://doi.org/10.1111/fcp.12819.

[29] L. Panneerselvam, A. Raghunath, M.S. Ravi, A. Vetrivel, V. Subramaniam, K. Sundarraj, E. Perumal, Ferulic acid attenuates arsenic-induced cardiotoxicity in rats, Biotechnol. Appl. Biochem. 67 (2020) 186–195, https://doi.org/10.1002/bab.1830.

[30] C. Ma, R. Xia, S. Yang, L. Liu, J. Zhang, K. Feng, Y. Shang, J. Qu, L. Li, N. Chen, S. Xu, W. Zhang, J. Mao, J. Han, Y. Chen, X. Yang, Y. Duan, G. Fan, Formononetin attenuates atherosclerosis via regulating interaction between KLF4 and SRA in apoE-/-mice, Theranostics 10 (2020) 1090–1106, https://doi.org/10.7150/thno.38115.

[31] L. Liu, R. Hu, H. You, J. Li, Y. Liu, Q. Li, X. Wu, J. Huang, X. Cai, M. Wang, L. Wei, Formononetin ameliorates muscle atrophy by regulating myostatin-mediated PI3K/Akt/FoxO3a pathway and satellite cell function in chronic kidney disease, J. Cell Mol. Med. 25 (2021) 1493–1506, https://doi.org/10.1111/jcmm.16238.

[32] S. Safarpour, M. Pirzadeh, A. Ebrahimpour, F. Shirafkan, F. Madani, M. Hosseini, A.A. Moghadamnia, S. Kazemi, Protective effect of kaempferol and its nanoparticles on 5-fluorouracil-induced cardiotoxicity in rats, BioMed Res. Int. 2022 (2022) 2273000, https://doi.org/10.1155/2022/2273000.

[33] C. Sun, T. Wang, C. Wang, Z. Zhu, X. Wang, J. Xu, H. An, The protective effect of kaempferol against ischemia/reperfusion injury through activating SIRT3 to inhibit oxidative stress, Braz. J. Cardiovasc. Surg. 37 (2022) 335–342, https://doi.org/10.21470/1678-9741-2020-0549.

[34] Z. Khan, N. Nath, A. Rauf, T.B. Emran, S. Mitra, F. Islam, D. Chandran, J. Barua, M.U. Khandaker, A.M. Idris, P. Wilairatana, M. Thiruvengadam, Multifunctional roles and pharmacological potential of β-sitosterol: emerging evidence toward clinical applications, Chem. Biol. Interact. 365 (2022) 110117, https://doi.org/10.1016/j.cbi.2022.110117.
[35] M. Sugimoto, R. Ko, H. Goshima, A. Koike, M. Shibano, K. Fujimori, Formononetin attenuates H2O2-induced cell death through decreasing ROS level by PI3K/Akt-Nrf2-activated antioxidant gene expression and suppressing MAPK-regulated apoptosis in neuronal SH-SY5Y cells, Neurotoxicology 85 (2021) 186–200, https://doi.org/10.1016/j.neuro.2021.05.014.
[36] B. Yang, C.Y. Zheng, R. Zhang, C. Zhao, S. Li, Y. An, Quercetin efficiently alleviates TNF-α-stimulated injury by signal transducer and activator of transcription 1 and mitogen-activated protein kinase pathway in H9c2 cells: a protective role of quercetin in myocarditis, J. Cardiovasc. Pharmacol. 77 (2021) 570–577, https://doi.org/10.1097/FJC.0000000000001000.
[37] G. Luo, L. Xiang, L. Xiao, Quercetin alleviates atherosclerosis by suppressing oxidized LDL-induced senescence in plaque macrophage via inhibiting the p38MAPK/p16 pathway, J. Nutr. Biochem. 116 (2023) 109314, https://doi.org/10.1016/j.jnutbio.2023.109314.
[38] H. Zhao, X. Zhang, M. Wang, Y. Lin, S. Zhou, Stigmasterol simultaneously induces apoptosis and protective autophagy by inhibiting akt/mTOR pathway in gastric cancer cells, Front. Oncol. 11 (2021) 629008, https://doi.org/10.3389/fonc.2021.629008.
[39] P. Rajendran, R.B. Ammar, F.J. Al-Saeedi, M.E. Mohamed, M.A. ElNaggar, S.Y. Al-Ramadan, G.M. Bekhet, A.M. Soliman, Kaempferol inhibits zearalenone-induced oxidative stress and apoptosis PI3K/Akt-Mediated Nrf2 signaling pathway: in vitro and in vivo studies, Int. J. Mol. Sci. 22 (2020) 217, https://doi.org/10.3390/ijms22010217.
[40] X. Ji, C. Zhang, J. Yang, Y. Tian, L. You, H. Yang, Y. Li, H. Liu, D. Pan, Z. Liu, Kaempferol improves exercise performance by regulating glucose Uptake, mitochondrial Biogenesis, and protein synthesis via PI3K/AKT and MAPK signaling pathways, Foods 13 (7) (2024) 1068, https://doi.org/10.3390/foods13071068.
[41] H. Cai, K. Li, Y. Yin, X. Ni, S. Xu, Quercetin alleviates DEHP exposure-induced pyroptosis and cytokine expression changes in grass carp L8824 cell line by inhibiting ROS/MAPK/NF-κB pathway, FISH &amp 143 (2023) 109223, https://doi.org/10.1016/j.fsi.2023.109223.
[42] X. Sun, G. Chen, Y. Xie, D. Jiang, J. Han, F. Chen, Y. Song, Qiliqiangxin improves cardiac function and attenuates cardiac remodelling in doxorubicin-induced heart failure rats, Pharm. Biol. 58 (2020) 417–426, https://doi.org/10.1080/13880209.2020.1761403.
[43] D. Zhang, A. Pan, J. Gu, R. Liao, X. Chen, Z. Xu, Upregulation of miR-144-3p alleviates Doxorubicin-induced heart failure and cardiomyocytes apoptosis via SOCS2/PI3K/AKT axis, Chem. Biol. Drug Des. 101 (2023) 24–39, https://doi.org/10.1111/cbdd.14104.
[44] X. Wu, X.F. Lv, X.D. Zhi, X.K. Zhao, Y.D. Li, Effects of Angelica Sinensis and Astragalus capsules on myocardial autophagy in rats with heart failure, The Chinese Journal of Clinical Pharmacology 40 (2024), 1453-1357.
[45] J. Li, X. Qin, W. Xu, H. Zhang, S. Huang, Y. Yang, M. Qin, Z. Mi, X. Zhong, Herb pair of Rhubarb-Astragalus mitigates renal interstitial fibrosis through downregulation of autophagy via p38-MAPK/TGF-β1 and p38-MAPK/smad2/3 pathways, Int. J. Biochem. Cell Biol. 169 (2024) 106549, https://doi.org/10.1016/j.biocel.2024.106549.
[46] C.Y. Cheng, H.C. Huang, S.T. Kao, Y.C. Lee, Angelica sinensis extract promotes neuronal survival by enhancing p38 MAPK-mediated hippocampal neurogenesis and dendritic growth in the chronic phase of transient global cerebral ischemia in rats, J. Ethnopharmacol. 278 (2021) 114301, https://doi.org/10.1016/j.jep.2021.114301.
[47] J. Mao, L. Tan, C. Tian, W. Wang, Y. Zou, Z. Zhu, Y. Li, Systematically investigate the mechanism underlying the therapeutic effect of Astragalus membranaceus in ulcerative colitis, Am. J. Med. Sci. 14 (2024) 1355–1357, https://doi.org/10.1016/j.amjms.2024.07.019.
[48] C. Cui, F.M. Yao, Clinical observation on modified Danggui Buxue decoction in the treatment of chronic heart failure with anemia, Chinese medicine modern distance education of china 19 (2021) 96–98.
[49] X. Wen, W. Huang, X.D. Han, Therapeutic efficacy of adding Angelica sinensis to replenish blood in treating patients with chronic heart failure with anaemia, Cardiovascular Disease Electronic Journal of integrated traditional Chinese and Western Medicine 8 (2020) 160–162.